⚜ Selected for a Viewpoint in *Physics*

P H Y S I C A L   R E V I E W   L E T T E R S

Large Cross-Phase Modulations at the Few-Photon Level

Zi-Yu Liu,[1] Yi-Hsin Chen,[2] Yen-Chun Chen,[1] Hsiang-Yu Lo,[1] Pin-Ju Tsai,[1] Ite A. Yu,[2,*]
Ying-Cheng Chen,[3] and Yong-Fan Chen[1,†]

[1]*Department of Physics, National Cheng Kung University, Tainan 70101, Taiwan*
[2]*Department of Physics and Frontier Research Center on Fundamental and Applied Sciences of Matters,
National Tsing Hua University, Hsinchu 30013, Taiwan*
[3]*Institute of Atomic and Molecular Sciences, Academia Sinica, Taipei 10617, Taiwan*
(Received 25 June 2016; published 7 November 2016)

We demonstrate an efficient cross-phase modulation (XPM) based on a closed-loop double-Λ system. The property of the double-Λ medium can be controlled by changing the phases of the applied optical fields. This phase-dependent XPM scheme can achieve large phase modulations at low-light intensities without requiring cavities or tightly focusing laser beams. With this scheme, we observe a π-level phase shift with two pulses, both consisting of eight photons in cold rubidium atoms. Such a novel scheme provides a simple route to generate strong interactions between photons and may have potential applications in all-optical quantum signal processing.

The realization of large cross-phase modulations (XPM) at low-light intensities, ultimately at the single-photon level, is an important but challenging task in quantum information science [1–3]. To reach this goal, one often requires high-finesse cavities to enhance nonlinear interactions between photons [4,5]. However, cavity-based experiments require many compromises such as balancing cavity bandwidth and light-matter coupling strength, which remain technical difficulties. Another promising approach for generating strong photon-photon interaction is electromagnetically induced transparency (EIT) [6–8], but according to the theoretical predictions by Harris and Hau, the cross-phase shift of the EIT-based Kerr medium in free space has an upper limit of order 0.1 radians at the single-photon level [9]. To date, EIT-based XPM on the order of microradians per photon has been observed in cold atoms [10,11] and an Rb-filled fiber system [12]. In recent years, to overcome this upper limit there have been many theoretical proposals and experimental studies on this subject, including double slow-light schemes [13,14], stationary light schemes [15,16], cavity EIT schemes [17,18], or Rydberg EIT schemes [19–25]. Very recently, two research teams have overcome this upper limit and observed single-photon cross-phase shifts of $\pi/3$ and π by using cavity EIT [26] and Rydberg EIT [27], respectively. This is great progress toward implementing a photon-photon gate.

Here, we report an experimental observation of a novel XPM scheme based on a phase-dependent double-Λ system. With this scheme, we observe a large cross-phase shift of 3.6 ± 1.0 radians induced by a light pulse containing around eight photons in cold rubidium atoms. This XPM scheme does not require cavities or Rydberg atoms, which provides a simple route to generate strong interactions between photons and obtain large cross-phase shifts per photon.

In the present study, we investigate a closed-loop double-Λ XPM in a laser-cooled ^{87}Rb atomic system, as depicted in Fig. 1(a). Cold atomic gas with an optical depth of approximately 50 is produced in a dark spontaneous-force optical trap [28]. A strong coupling field (Ω_c denotes its Rabi frequency) drives the $|2\rangle \leftrightarrow |3\rangle$ transition to create a transparent medium for a weak probe pulse (Ω_p, $|1\rangle \leftrightarrow |3\rangle$) through quantum interference. The coupling and probe fields form the first Λ-type EIT system. The second Λ-type
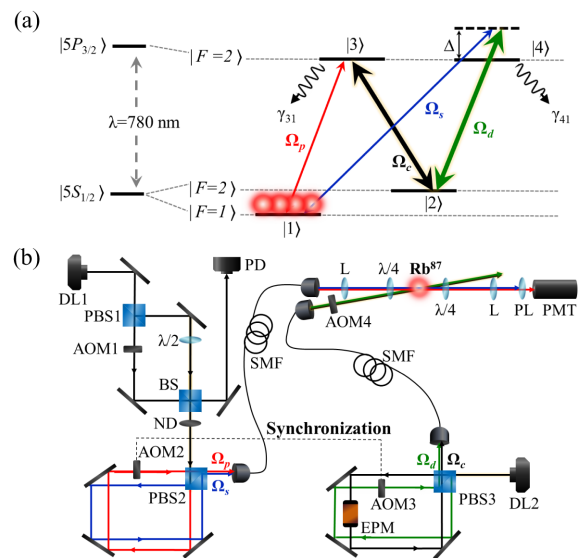

FIG. 1. Energy level scheme and experimental apparatus. (a) Energy levels of the ^{87}Rb D_2-line transition for the double-Λ experiment. Signal detuning Δ is defined as $\omega_s - \omega_{24}$, where ω_s and ω_{24} are the frequencies of the signal field and the $|2\rangle \leftrightarrow |4\rangle$ transition, respectively. (b) Schematic diagram of the experimental setup. DL, diode laser; $\lambda/4$, quarter wave plate; $\lambda/2$, half wave plate; PL, polarizer; ND, neutral density filter; L, lens.

EIT system is created by a strong driving field (Ω_d, $|2\rangle \leftrightarrow |4\rangle$) and a weak signal pulse (Ω_s, $|1\rangle \leftrightarrow |4\rangle$). In the experiment, the coupling and probe fields are right circularly polarized ($\sigma+$) while the driving and signal fields are left circularly polarized ($\sigma-$). The four laser fields drive the D_2-line transition of the ^{87}Rb atoms to form the closed-loop double-Λ EIT system, as shown in Fig. 1(a).

A schematic diagram of the experimental setup is shown in Fig. 1(b). The probe and signal fields are produced using a single diode laser (DL1); the coupling and driving fields are produced using another diode laser (DL2). DL2 is directly injection locked using an external cavity diode laser (TOPTICA DL 100) with a laser linewidth of around 1 MHz. One beam from the external cavity diode laser is sent through a 6.8-GHz electro-optic modulator (EOM, New Focus 4851). DL1 is injection locked by an intermediate laser seeded with the high-frequency sideband of the EOM output. The above arrangement is capable of completely eliminating the influence of the carrier of the EOM output on DL1. The probe beam is overlapped with the signal beam on a polarization beam splitter (PBS2) and then sent to a single-mode fiber (SMF) to obtain the optimal spatial mode matching. The e^{-2} diameters of the probe (signal) and coupling (driving) beams are 0.2 and 3 mm, respectively. These two beams propagate at an angle of around 1°. All of the laser fields are switched on and off via acousto-optic modulators (AOMs). We utilize AOM1 to control the widths of the probe and signal pulses. The coupling and driving fields are switched on and off via AOM4 [see Fig. 1(b)]. The experimental data are detected by a photomultiplier tube module (PMT, Hamamatsu H6780-20 and C9663) with a conversion gain of around 9×10^7 V/W and then recorded using an oscilloscope (Agilent MSO6034A) throughout the experiment. The number of photons of the few-photon pulses (probe and signal pulses) are also checked by a single-photon counting module (Perkin-Elmer SPCM-AQR-13).

When conducting the phase-dependent double-Λ experiment, an electro-optic phase modulator (EPM, Thorlabs EO-PM-NR-C1) is applied to vary the phase of the coupling field (Ω_c). Furthermore, to stabilize the relative phase of the four laser fields, two main setups are utilized in this experiment. (i) The optical paths of the probe and signal (coupling and driving) fields are arranged in the configuration of a Sagnac-like interferometer to reduce the path fluctuations between these two beams, as shown in Fig. 1(b). (ii) AOM2 and AOM3 are driven by the same rf generator through an rf power splitter (Mini-Circuits ZMSC-2-1+).

We utilize a sensitive beat-note interferometer to measure the cross-phase shift of the weak probe pulse. The probe beam is first split into the transmitted and reflected beams by PBS1 in order to establish the beat-note interferometer [see Fig. 1(b)]. The transmitted beam passes through the AOM1, which has a driving frequency of 80 MHz, to generate a first-order beam for the probe pulse and then recombines with the

reflected beam from the PBS1 on a beam splitter (BS). One beam from the BS is called the reference beat notes, which is directly received by a photodetector (PD, New Focus 1801). The other beam, corresponding to the probe beat notes, is detected by a PMT after propagating through the double-Λ medium. The phase shift of the probe pulse is measured by directly comparing the reference and probe beat notes. In this experiment, only the phase shift within 1 μs of the end of the probe pulse is measured in order to acquire the steady-state results. The probe transmission is simultaneously obtained from the amplitude of the probe beat notes. The experimental setup and details of the beat-note interferometer can be found in Ref. [29].

To theoretically analyze the behavior of the probe and signal pulses propagating in the double-Λ EIT medium, we use the Maxwell-Schrödinger equations below:

$$\frac{\partial \Omega_p}{\partial z} + \frac{1}{c}\frac{\partial \Omega_p}{\partial t} = i\frac{\alpha_p \gamma_{31}}{2L}\rho_{31}, \tag{1}$$

$$\frac{\partial \Omega_s}{\partial z} + \frac{1}{c}\frac{\partial \Omega_s}{\partial t} = i\frac{\alpha_s \gamma_{41}}{2L}\rho_{41}, \tag{2}$$

where $\Omega_p = |\Omega_p|e^{i\phi_p}$ and $\Omega_s = |\Omega_s|e^{i\phi_s}$ are the Rabi frequencies of the probe and signal pulses, respectively. ϕ_p (ϕ_s) describes the phase information carried by the probe (signal) pulse. ρ_{31} (ρ_{41}) is the slowly varying amplitude of the optical coherence of the probe (signal) transition. $\alpha_p = n\sigma_{13}L$ ($\alpha_s = n\sigma_{14}L$) represents the optical depth of the probe (signal) transition, where n is the number density of the atoms, σ_{13} (σ_{14}) is the atomic absorption cross section of the probe (signal) transition, and L is the optical path length of the medium. γ_{31} and γ_{41} represent the total coherence decay rates from the $|3\rangle$ and $|4\rangle$ excited states, respectively. We note that the optical depths of the probe and signal transitions in this experiment are the same ($\alpha_p = \alpha_s$) because σ_{13} is equal to σ_{14} by considering three degenerate Zeeman sublevels, as shown in Fig. 1(a).

In the case where the probe and signal fields are very weak (i.e., $\rho_{11} \simeq 1$), the optical Bloch equations of the slowly varying amplitudes of the density-matrix elements are given by

$$\frac{d}{dt}\rho_{41} = \frac{i}{2}\Omega_s + \frac{i}{2}\Omega_d\rho_{21} + \left(i\Delta - \frac{\gamma_{41}}{2}\right)\rho_{41}, \tag{3}$$

$$\frac{d}{dt}\rho_{31} = \frac{i}{2}\Omega_p + \frac{i}{2}\Omega_c\rho_{21} - \frac{\gamma_{31}}{2}\rho_{31}, \tag{4}$$

$$\frac{d}{dt}\rho_{21} = \frac{i}{2}\Omega_c^*\rho_{31} + \frac{i}{2}\Omega_d^*\rho_{41} - \frac{\gamma_{21}}{2}\rho_{21}, \tag{5}$$

where $\Omega_c = |\Omega_c|e^{i\phi_c}$ and $\Omega_d = |\Omega_d|e^{i\phi_d}$ are the Rabi frequencies of the coupling and driving transitions, respectively. ϕ_c (ϕ_d) describes the phase information carried by the coupling (driving) field. Δ denotes the detuning of the

signal transition [see Fig. 1(a)]. γ_{21} represents the dephasing rate of the $|1\rangle$ and $|2\rangle$ ground states. Each parameter in the theoretical model is individually determined from additional experiments as follows: $|\Omega_c|$ is determined from the separation of the two absorption peaks in the EIT spectrum. $|\Omega_d|$ is determined from the EIT-based photon-switching effect [30]. α_p is derived from the delay time of the slow-light pulse [31]. γ_{21} is $0.0010(2)\Gamma$, as estimated by the degree of EIT transparency. $\Gamma = 2\pi \times 6$ MHz is the spontaneous decay rate of the excited states. γ_{31} and γ_{41} are both $1.25(2)\Gamma$, contributed mostly by the spontaneous decay rate and laser linewidth, as obtained from the spectral width of the one-photon absorption. Assuming $\gamma_{21} = 0$, $\gamma_{31} = \gamma_{41}$, and $\alpha_p = \alpha_s = \alpha$, the steady-state solutions of Eqs. (1)–(5) for the probe and signal fields are

$$\Omega_p(\alpha) = \frac{1}{|\Omega|^2}[|\Omega_c|^2\Omega_p(0) + \Omega_c\Omega_d^*\Omega_s(0)]$$
$$+ \frac{1}{|\Omega|^2}[|\Omega_d|^2\Omega_p(0) - \Omega_c\Omega_d^*\Omega_s(0)]e^{-i(\alpha/2\xi)}, \quad (6)$$

$$\Omega_s(\alpha) = \frac{1}{|\Omega|^2}[|\Omega_d|^2\Omega_s(0) + \Omega_d\Omega_c^*\Omega_p(0)]$$
$$+ \frac{1}{|\Omega|^2}[|\Omega_c|^2\Omega_s(0) - \Omega_d\Omega_c^*\Omega_p(0)]e^{-i(\alpha/2\xi)}, \quad (7)$$

where $|\Omega|^2 = |\Omega_c|^2 + |\Omega_d|^2$, $\xi = i + 2(|\Omega_c|^2\Delta/|\Omega|^2\gamma_{31})$. The terms $\Omega_p(0)$ and $\Omega_s(0)$ represent the incident probe and signal fields, respectively. Under the conditions of $|\Omega_c| = |\Omega_d|$ and $|\Omega_p(0)| = |\Omega_s(0)|$, we obtain simple steady-state solutions for the probe and signal fields as follows:

$$\frac{\Omega_p(\alpha)}{\Omega_p(0)} = \frac{1}{2}[1 + e^{-i\phi_r} + (1 - e^{-i\phi_r})e^{-i(\alpha/2\xi)}], \quad (8)$$

$$\frac{\Omega_s(\alpha)}{\Omega_s(0)} = \frac{1}{2}[1 + e^{i\phi_r} + (1 - e^{i\phi_r})e^{-i(\alpha/2\xi)}], \quad (9)$$

where the relative phase of the four laser fields ϕ_r is defined as $\phi_p - \phi_c + \phi_d - \phi_s$. According to Eqs. (8) and (9), when $\Delta = 0$ and $\phi_r = 0$, the double-Λ medium becomes completely transparent for both the probe and the signal fields. On the other hand, when $\phi_r = \pi$, the medium becomes opaque and has maximum attenuation for both the probe and the signal fields. This phase-dependent double-Λ system with $\Delta = 0$ can be applied in all-optical switching, as previously described [32]. Here, we focus on demonstrating large phase modulations at low-light intensities with this scheme. Of note, the matched propagation of a pair of slow-light pulses in the double-Λ medium has been theoretically discussed in Ref. [33]. Also, interference between multiple Λ transitions has been studied in Refs. [34,35]. Recently, broadly tunable light phase modulations at low-light intensities via the phase-resonant closed-loop optical transitions have been theoretically studied in Ref. [36].

We first measure the transmission of a probe pulse propagating through a three-level Λ-type EIT medium. After all of the lasers and magnetic fields of the dark spontaneous-force optical trap are turned off and the coupling field (Ω_c) is switched on for 100 μs, the 10-μs probe square pulse is switched on to perform the measurement. The experiment is conducted at a repetition rate of 100 Hz. The input power of the probe pulse is set to around 1 nW in the EIT experiment. The Rabi frequency of the coupling transition $|\Omega_c|$ is 0.7Γ, corresponding to the coupling laser power of around 0.5 mW. Figure 2 shows the probe transmission as a function of probe detuning. The inset shows the EIT transmission window. The measurement data (circles) are in good agreement with the theoretical curve (red line). The theoretical curve is plotted using the EIT theoretical expression in Ref. [29].

Next, we perform the double-Λ experiment in the pulsed regime. Figure 3 shows typical experimental data, where $\alpha_p = 46$, $\Delta = 13\Gamma$, $|\Omega_c| = |\Omega_d| = 0.7\Gamma$, and the input powers of both the probe and the signal pulses are set to around 1 nW, corresponding to $|\Omega_p(0)| = |\Omega_s(0)| \approx 0.016\Gamma$ (i.e., $|\Omega_{p(s)}(0)| \ll |\Omega_{c(d)}|$). Here, the widths of both the probe and signal pulses are set to 10 μs. We utilized the EPM to vary the relative phase ϕ_r [see Fig. 1(b)]. The relative phase ϕ_r is set to 1.5 radians in Fig. 3(a) and 4.5 radians in Fig. 3(b). The solid and dashed lines represent the experimental data and theoretical curves, respectively. The theoretical curves are plotted by numerically solving Eqs. (1)–(5). The black (green) lines are the input probe (signal) pulses, and the blue (red) lines are the transmitted probe (signal) pulses. The group-velocity mismatch of the transmitted probe and signal pulses in Fig. 3 is due to $\Delta \neq 0$. The experimental data
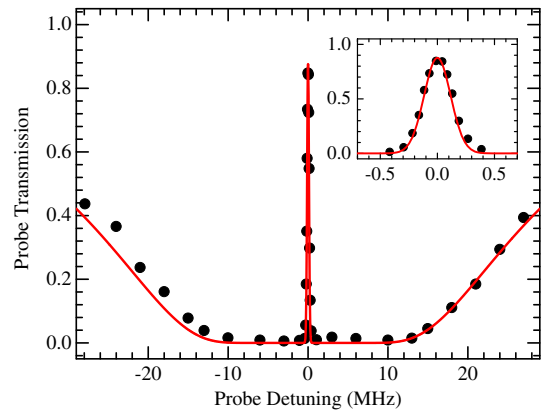

FIG. 2. Observed EIT transmission versus probe field detuning. The black circles and red line represent the measurement data and theoretical curve, respectively. The inset shows the EIT transmission window. Probe detuning is defined as $\omega_p - \omega_{13}$, where ω_p and ω_{13} are the frequencies of the probe field and the $|1\rangle \leftrightarrow |3\rangle$ transition, respectively. The parameters for the theoretical curve are $\alpha_p = 52$, $|\Omega_c| = 0.7\Gamma$, $\gamma_{21} = 0.001\Gamma$, and $\gamma_{31} = \gamma_{41} = 1.25\Gamma$.
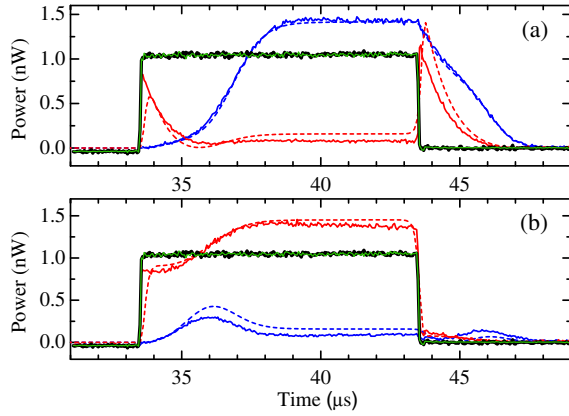
FIG. 3. Phase-dependent double-Λ experiment in the pulsed regime. The solid and dashed lines represent the experimental data and theoretical curves, respectively. The black (green) lines are the input probe (signal) pulses; the blue (red) lines are the transmitted probe (signal) pulses. The parameters for the theoretical curves (dashed lines) are $\alpha_p = 46$, $|\Omega_c| = |\Omega_d| = 0.7\Gamma$, $\Delta = 13\Gamma$, $\gamma_{21} = 0.001\Gamma$, and $\gamma_{31} = \gamma_{41} = 1.25\Gamma$. (a) The relative phase $\phi_r = 1.5$ rad. (b) $\phi_r = 4.5$ rad. The peak powers of both the probe and signal pulses are around 1 nW, corresponding to around 40 000 photons per pulse.

FIG. 4. Phase modulations at the few-photon level. Dependence of the transmission and the phase shift of the probe pulse on the relative phase ϕ_r. The numbers of both the probe and the signal photons are around 400 in (a) and (b), 40 in (c) and (d), and 8 in (e) and (f). Circles (squares) represent the transmission (phase shift) of the probe pulse. The black lines are the theoretical curves of the probe transmission and phase shift. The parameters for the theoretical curves are $\alpha_p = 50$, $|\Omega_c| = |\Omega_d| = 0.7\Gamma$, $\Delta = 13\Gamma$, $\gamma_{21} = 0.001\Gamma$, and $\gamma_{31} = \gamma_{41} = 1.25\Gamma$.

also show that the power of the transmitted light exceeds its input power in the double-Λ system. This light-amplification phenomenon is caused by the coherent light transfer between two N-type four-wave-mixing processes ($|1\rangle \rightarrow |3\rangle \rightarrow |2\rangle \rightarrow |4\rangle \rightarrow |1\rangle$ and $|1\rangle \rightarrow |4\rangle \rightarrow |2\rangle \rightarrow |3\rangle \rightarrow |1\rangle$) [37]. More detailed discussions on the coherent light amplification can be found in the Supplemental Material [38].

Figure 4 shows the experimental data of the double-Λ-based XPM at low-light levels. The experimental parameters are the same as those in Fig. 3 except for the optical depth ($\alpha_p = 50$). We first perform the double-Λ experiment where the input powers of both the probe and the signal pulses are set to 10 pW, corresponding to around 400 photons per pulse. Figures 4(a) and 4(b) show the experimental data of the dependence of the probe transmission and phase shift on the relative phase ϕ_r, respectively, which are in agreement with the theoretical curves. We subsequently perform the double-Λ experiment at the few-photon level. The input powers of both the probe and the signal pulses in Figs. 4(c) and 4(e) are reduced to around 1 and 0.2 pW, corresponding to around 40 and 8 photons, respectively. Circles (squares) represent the experimental data of the probe transmission (phase shift). The black lines are the theoretical curves of the probe transmission and phase shift. Throughout the experiment, the statistical error bar is evaluated using six samples. Each sample is averaged 4096, 16 384, and 32 768 times for the measurement with 400, 40, and 8 incident photons, respectively. All error bars in this Letter represent a statistical uncertainty of one standard deviation. We emphasize that only under the
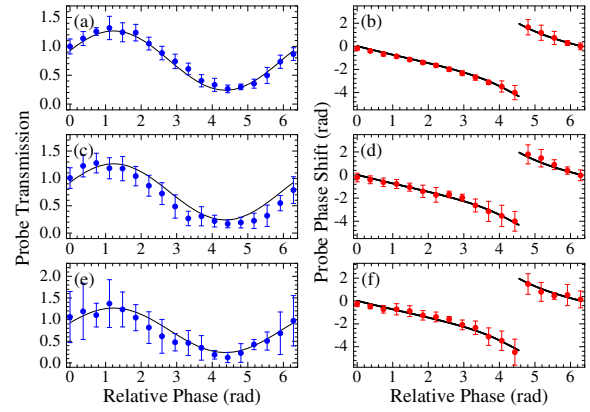
condition of $|\Omega_c| = |\Omega_d|$ and $|\Omega_p(0)| = |\Omega_s(0)|$, the probe transmission and phase modulation after propagating through the double-Λ medium are the same according to Eqs. (8) and (9). If the intensity of any one of the four applied fields is changed in Fig. 4, and other parameters remain constant, the transmission and phase modulation would change according to Eqs. (6) and (7). In other words, the double-Λ XPM scheme not only depends on the relative phase but also on the field intensity. A detailed theoretical analysis can be found in the Supplemental Material [38].

As the number of the probe and signal photons decreases, the error bars of the measurement data become large due to smaller signal-to-noise ratios, as shown in Fig. 4. Although the data in Fig. 4(f) possess a large amount of phase noise of around 1 radian, the measured values are still valid considering the considerable phase shift. For instance, in Fig. 4(f), a maximum phase shift of -4.5 ± 0.9 radians is measured when the relative phase ϕ_r is set to 4.4 radians. When the signal pulse is absent, we also measure the probe phase shift of -0.9 ± 0.1 radians, which is consistent with the theoretical predictions. Hence, we conclude that a cross-phase shift of 3.6 ± 1.0 radians induced by a light pulse containing around eight photons has been realized with this scheme. For practicality in optical and quantum control, a π-order XPM with high-light transmission is important. However, the probe transmission is around 20% in the experiment of Fig 4. Therefore, achieving a π-order XPM with high-light transmission via the current scheme remains a considerable challenge. A detailed theoretical analysis can be found in the Supplemental Material [38]. So far, we do not perform the experiment using few-photon pulses containing less

than eight photons because the long-term instability of our experimental system prevents us from improving the signal-to-noise ratios by collecting more data. In principle, this phase-dependent XPM scheme can reach the goal of π phase modulation per photon if one can prepare two phase-coherent single-photon pulses to be as the probe and signal pulses.

In conclusion, we have demonstrated an efficient XPM based on a closed-loop double-Λ system. The property of the double-Λ medium can be controlled by changing the phases of the applied optical fields. This phase-dependent XPM scheme can achieve large phase modulations at low-light intensities without requiring cavities or Rydberg atoms. We have observed a cross-phase shift of 3.6 ± 1.0 radians induced by a light pulse containing eight photons in cold ^{87}Rb atoms with this scheme. Such a novel scheme provides a simple route to generate strong interaction between photons and may have potential applications in all-optical quantum signal processing.

---

*yu@phys.nthu.edu.tw
†yfchen@mail.ncku.edu.tw

[1] D. Bouwmeester, A. Ekert, and A. Zeilinger, *The Physics of Quantum Information* (Springer, New York, 2000).

[2] M. A. Nielsen and I. L. Chuang, *Quantum Computation and Quantum Information* (Cambridge University Press, Cambridge, England, 2000).

[3] N. Imoto, H. A. Haus, and Y. Yamamoto, Phys. Rev. A **32**, 2287 (1985).

[4] Q. A. Turchette, C. J. Hood, W. Lange, H. Mabuchi, and H. J. Kimble, Phys. Rev. Lett. **75**, 4710 (1995).

[5] I. Fushman, D. Englund, A. Faraon, N. Stoltz, P. Petroff, and J. Vučković, Science **320**, 769 (2008).

[6] S. E. Harris, Phys. Today **50**, No. 7, 36 (1997).

[7] M. D. Lukin, Rev. Mod. Phys. **75**, 457 (2003).

[8] M. Fleischhauer, A. Imamoğlu, and J. P. Marangos, Rev. Mod. Phys. **77**, 633 (2005).

[9] S. E. Harris and L. V. Hau, Phys. Rev. Lett. **82**, 4611 (1999).

[10] H.-Y. Lo, Y.-C. Chen, P.-C. Su, H.-C. Chen, J.-X. Chen, Y.-C. Chen, I. A. Yu, and Y.-F. Chen, Phys. Rev. A **83**, 041804(R) (2011).

[11] A. Feizpour, M. Hallaji, G. Dmochowski, and A. M. Steinberg, Nat. Phys. **11**, 905 (2015).

[12] V. Venkataraman, K. Saha, and L. Gaeta, Nat. Photonics **7**, 138 (2012).

[13] M. D. Lukin and A. Imamoğlu, Phys. Rev. Lett. **84**, 1419 (2000).

[14] B.-W. Shiau, M.-C. Wu, C.-C. Lin, and Y.-C. Chen, Phys. Rev. Lett. **106**, 193006 (2011).

[15] M. Bajcsy, A. S. Zibrov, and M. D. Lukin, Nature (London) **426**, 638 (2003).

[16] Y.-H. Chen, M.-J. Lee, W. Hung, Y.-C. Chen, Y.-F. Chen, and I. A. Yu, Phys. Rev. Lett. **108**, 173603 (2012).

[17] M. Mücke, E. Figueroa, J. Bochmann, C. Hahn, K. Murr, S. Ritter, C. J. Villas-Boas, and G. Rempe, Nature (London) **465**, 755 (2010).

[18] Y. Zhu, Opt. Lett. **35**, 303 (2010).

[19] I. Friedler, D. Petrosyan, M. Fleischhauer, and G. Kurizki, Phys. Rev. A **72**, 043803 (2005).

[20] A. K. Mohapatra, T. R. Jackson, and C. S. Adams, Phys. Rev. Lett. **98**, 113003 (2007).

[21] J. D. Pritchard, D. Maxwell, A. Gauguet, K. J. Weatherill, M. P. A. Jones, and C. S. Adams, Phys. Rev. Lett. **105**, 193603 (2010).

[22] A. V. Gorshkov, J. Otterbach, M. Fleischhauer, T. Pohl, and M. D. Lukin, Phys. Rev. Lett. **107**, 133602 (2011).

[23] B. He, A. V. Sharypov, J. Sheng, C. Simon, and M. Xiao, Phys. Rev. Lett. **112**, 133606 (2014).

[24] S. Baur, D. Tiarks, G. Rempe, and S. Dürr, Phys. Rev. Lett. **112**, 073901 (2014).

[25] H. Gorniaczyk, C. Tresp, J. Schmidt, H. Fedder, and S. Hofferberth, Phys. Rev. Lett. **113**, 053601 (2014).

[26] K. M. Beck, M. Hosseini, Y. Duan, and V. Vuletić, Proc. Natl. Acad. Sci. U.S.A. **113**, 9740 (2016).

[27] D. Tiarks, S. Schmidt, G. Rempe, and S. Dürr, Sci. Adv. **2**, e1600036 (2016).

[28] W. Ketterle, K. B. Davis, M. A. Joffe, A. Martin, and D. E. Pritchard, Phys. Rev. Lett. **70**, 2253 (1993).

[29] H.-Y. Lo, P.-C. Su, Y.-W. Cheng, P.-I Wu, and Y.-F. Chen, Opt. Express **18**, 18498 (2010).

[30] Y.-F. Chen, Z.-H. Tsai, Y.-C. Liu, and I. A. Yu, Opt. Lett. **30**, 3207 (2005).

[31] L. V. Hau, S. E. Harris, Z. Dutton, and C. H. Behroozi, Nature (London) **397**, 594 (1999).

[32] H. Kang, G. Hernandez, J. Zhang, and Y. Zhu, Phys. Rev. A **73**, 011802(R) (2006).

[33] L. Deng and M. G. Payne, Phys. Rev. A **71**, 011803(R) (2005).

[34] G. Campbell, A. Ordag, and A. I. Lvovsky, New J. Phys. **11**, 103021 (2009).

[35] G. Campbell, M. Hosseine, B. M. Sparkes, P. K. Lam, and B. C. Buchler, New J. Phys. **14**, 033022 (2012).

[36] M. Artoni and A. Zavatta, Phys. Rev. Lett. **115**, 113005 (2015).

[37] C.-K. Chiu, Y.-H. Chen, Y.-C. Chen, I. A. Yu, Y.-C. Chen, and Y.-F. Chen, Phys. Rev. A **89**, 023839 (2014).

[38] See Supplemental Material at http://link.aps.org/supplemental/10.1103/PhysRevLett.117.203601, which includes Ref. [39], for a detailed theoretical analysis.

[39] E. A. Korsunsky and D. V. Kosachiov, Phys. Rev. A **60**, 4996 (1999).